

Supporting Information

Construction of rare-earth-modified layered double hydroxide heterostructures and enhancement of overall water splitting efficiency

Yuhan He^a, Yaohui Jin^a, Ming Lu^d, Yuanyuan Wu^a, Wei Jiang^{ab}, Xingjing Zhang^a, Yantao Sun^{a*}, Xianyu Chu^{abd*}, Guangbo Che^{c*} and Chunbo Liu^{ab*}

^a Key Laboratory of Preparation and Application of Environmental Friendly Materials of the Ministry of Education, Jilin Normal University, Changchun, 130103, P. R. China.

^b Jilin Joint Technology Innovation Laboratory of Developing and Utilizing Materials of Reducing Pollution and Carbon Emissions, College of Engineering, Jilin Normal University, Siping, 136000, P. R. China.

^c Jilin Provincial Key Laboratory of Western Jilin's Clean Energy, Baicheng Normal University, Baicheng 137000, P. R. China.

^d The Joint Laboratory of MXene Materials, Key Laboratory of Functional Materials Physics and Chemistry of the Ministry of Education, Jilin Normal University, Changchun, 130103, P. R. China.

*Corresponding author.

E-mail addresses:

syt0307021@jlnu.edu.cn (Y. Sun), chuxy22@jlnu.edu.cn (X. Chu),
guangboche@bcnu.edu.cn (G. Che) and chunboliu@jlnu.edu.cn (C. Liu)

Contents

Figures

Figure S1. SEM images of (A) $\text{TiO}_2@\text{C}$, (B) CoCe-LDH, (C) $\text{Co}_{0.1}\text{Ce}_{0.1}\text{-LDH-TiO}_2@\text{C}$, (D) $\text{Co}_{0.1}\text{Ce}_{0.05}\text{-LDH-TiO}_2@\text{C}$, (E) $\text{Co}_{0.1}\text{Ce}_{0.005}\text{-LDH-TiO}_2@\text{C}$, (F) $\text{Co}_{0.1}\text{Ce}_{0.001}\text{-LDH-TiO}_2@\text{C}$.

Figure S2. TEM images of (A) $\text{TiO}_2@\text{C}$, (B) CoCe-LDH.

Figure S3. The EDS spectrum of a (A) $\text{Co}_{0.1}\text{Ce}_{0.1}\text{-LDH-TiO}_2@\text{C}$, (B) $\text{Co}_{0.1}\text{Ce}_{0.05}\text{-LDH-TiO}_2@\text{C}$, (C) $\text{Co}_{0.1}\text{Ce}_{0.01}\text{-LDH-TiO}_2@\text{C}$, (D) $\text{Co}_{0.1}\text{Ce}_{0.005}\text{-LDH-TiO}_2@\text{C}$, (E) $\text{Co}_{0.1}\text{Ce}_{0.001}\text{-LDH-TiO}_2@\text{C}$.

Figure S4. SAED image of $\text{Co}_{0.1}\text{Ce}_{0.01}\text{-LDH-TiO}_2@\text{C}$.

Figure S5. CV of (A) $\text{TiO}_2@\text{C}$, (B) CoCe-LDH and (C) $\text{Co}_{0.1}\text{Ce}_{0.01}\text{-LDH-TiO}_2@\text{C}$ at various scan rates for HER.

Figure S6. CV of (A) $\text{TiO}_2@\text{C}$, (B) CoCe-LDH and (C) $\text{Co}_{0.1}\text{Ce}_{0.01}\text{-LDH-TiO}_2@\text{C}$ at various scan rates for OER.

Figure S7. Chronopotentiometry measurement of CoCe-LDH of (A) HER and (B) OER performance.

Figure S8. Stepped current stability test of $\text{Co}_{0.1}\text{Ce}_{0.01}\text{-LDH-TiO}_2@\text{C}$ for (A) HER and (C) OER, LSV curve comparison experiment before and after CV cycling of $\text{Co}_{0.1}\text{Ce}_{0.01}\text{-LDH-TiO}_2@\text{C}$ for (B) HER and (D) OER.

Figure S9. LSV polarization curves under different electrolyte temperatures of (A-B) CoCe-LDH.

Figure S10. The SEM images of $\text{Co}_{0.1}\text{Ce}_{0.01}\text{-LDH-TiO}_2@\text{C}$ after (A) HER and (B) OER.

Figure S11. LSV polarization curves at high current density of $\text{Co}_{0.1}\text{Ce}_{0.01}\text{-LDH-TiO}_2@\text{C}$ for (A) HER and (B) OER.

Tables

Table S1. EIS parameters of $\text{TiO}_2@\text{C}$, CoCe-LDH and $\text{Co}_{0.1}\text{Ce}_{0.01}\text{-LDH-TiO}_2@\text{C}$ at different potentials for HER.

Table S2. EIS parameters of $\text{TiO}_2@\text{C}$, CoCe-LDH and $\text{Co}_{0.1}\text{Ce}_{0.01}\text{-LDH-TiO}_2@\text{C}$ at different potentials for OER.

Table S3. Comparison of HER and OER performance for $\text{Co}_{0.1}\text{Ce}_{0.01}\text{-LDH-TiO}_2@\text{C}$ with other similar catalysts.

Table S4. Comparison of the stability performance of $\text{Co}_{0.1}\text{Ce}_{0.01}\text{-LDH-TiO}_2@\text{C}$ with other

catalysts for OER.

Table S5. Comparison of the stability performance of $\text{Co}_{0.1}\text{Ce}_{0.01}\text{-LDH-TiO}_2\text{@C}$ with other catalysts for overall water splitting.

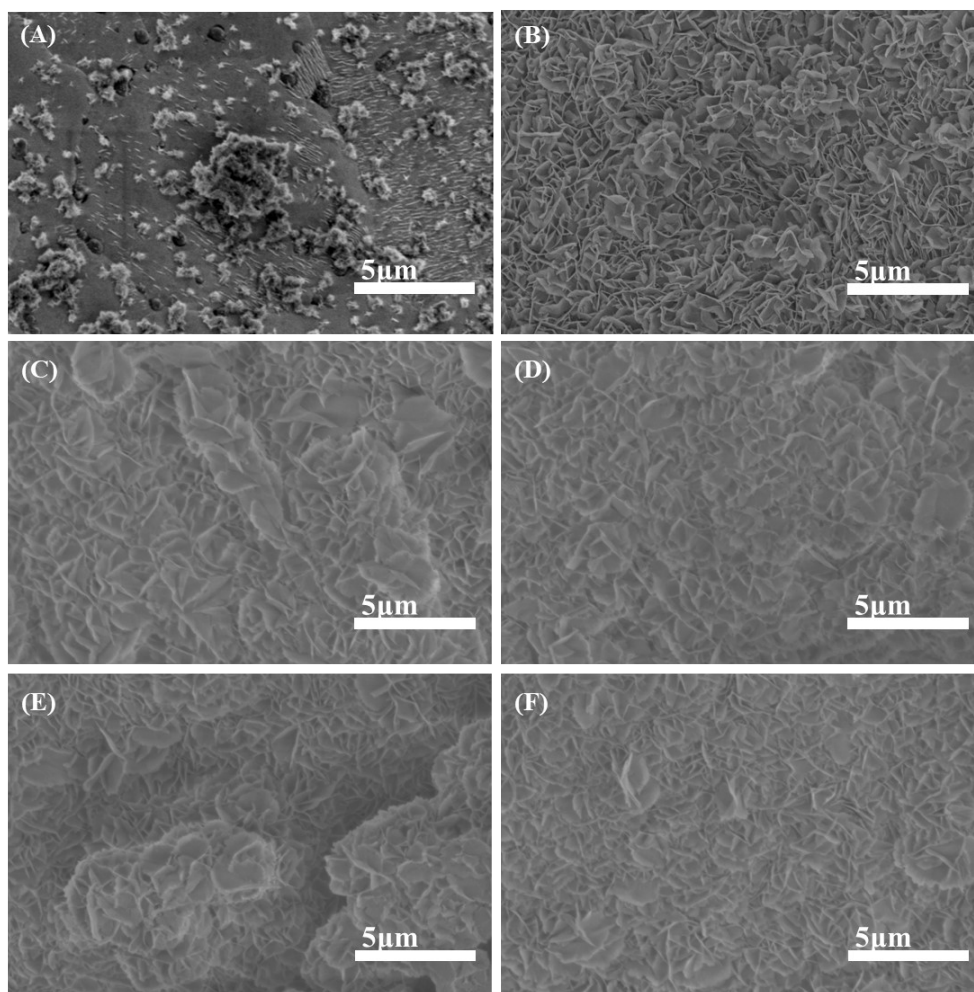


Figure S1. SEM images of (A) $\text{TiO}_2@\text{C}$, (B) CoCe-LDH , (C) $\text{Co}_{0.1}\text{Ce}_{0.1}\text{-LDH-TiO}_2@\text{C}$, (D) $\text{Co}_{0.1}\text{Ce}_{0.05}\text{-LDH-TiO}_2@\text{C}$, (E) $\text{Co}_{0.1}\text{Ce}_{0.005}\text{-LDH-TiO}_2@\text{C}$, (F) $\text{Co}_{0.1}\text{Ce}_{0.001}\text{-LDH-TiO}_2@\text{C}$.

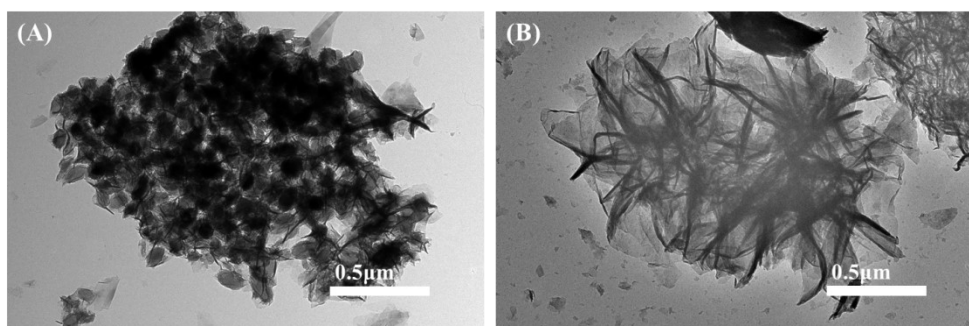


Figure S2. TEM images of (A) TiO₂@C, (B) CoCe-LDH.

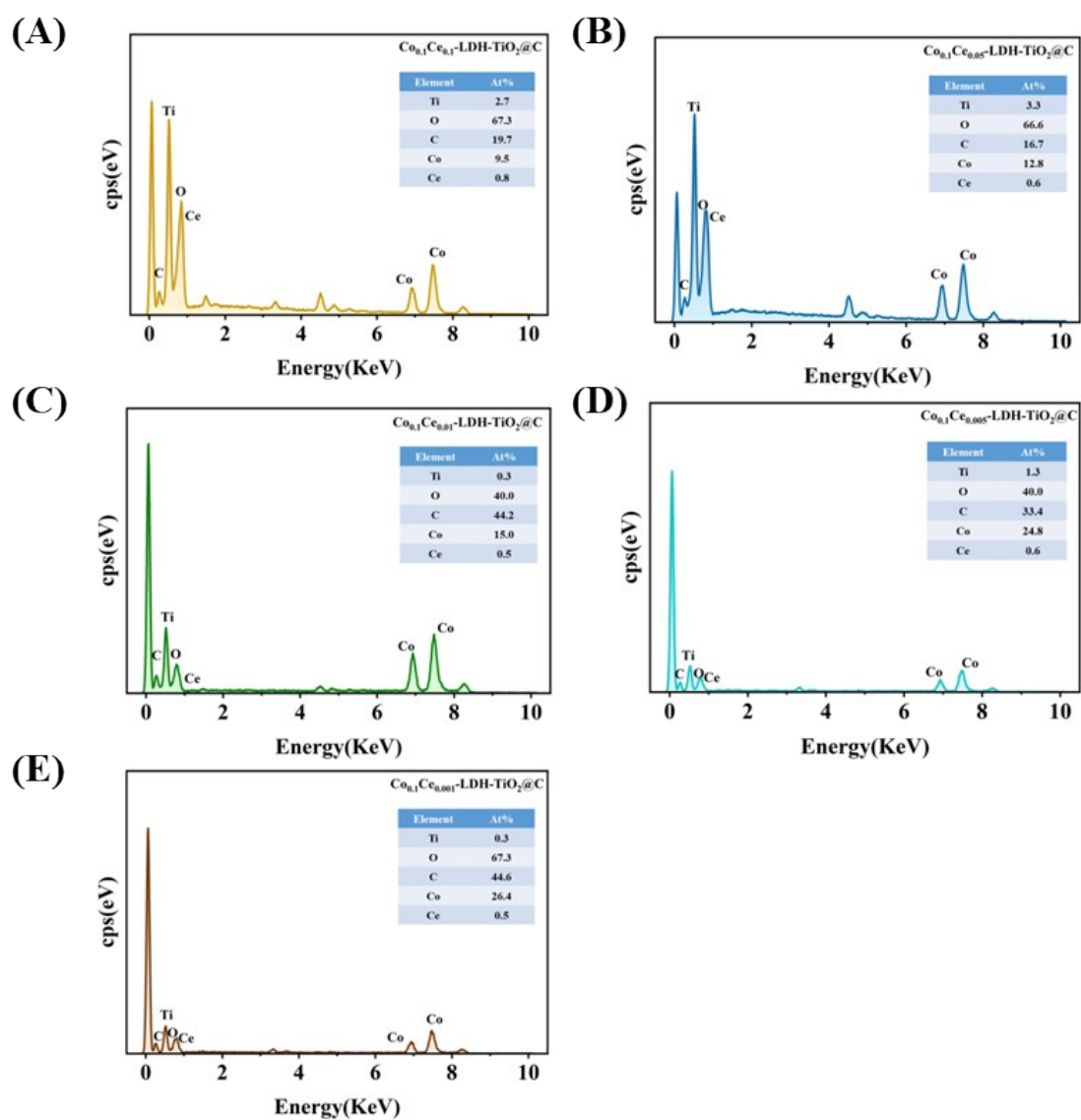


Figure S3. The EDS spectrum of aa (A) $\text{Co}_{0.1}\text{Ce}_{0.1}\text{-LDH-TiO}_2\text{@C}$, (B) $\text{Co}_{0.1}\text{Ce}_{0.05}\text{-LDH-TiO}_2\text{@C}$, (C) $\text{Co}_{0.1}\text{Ce}_{0.01}\text{-LDH-TiO}_2\text{@C}$, (D) $\text{Co}_{0.1}\text{Ce}_{0.005}\text{-LDH-TiO}_2\text{@C}$, (E) $\text{Co}_{0.1}\text{Ce}_{0.001}\text{-LDH-TiO}_2\text{@C}$.

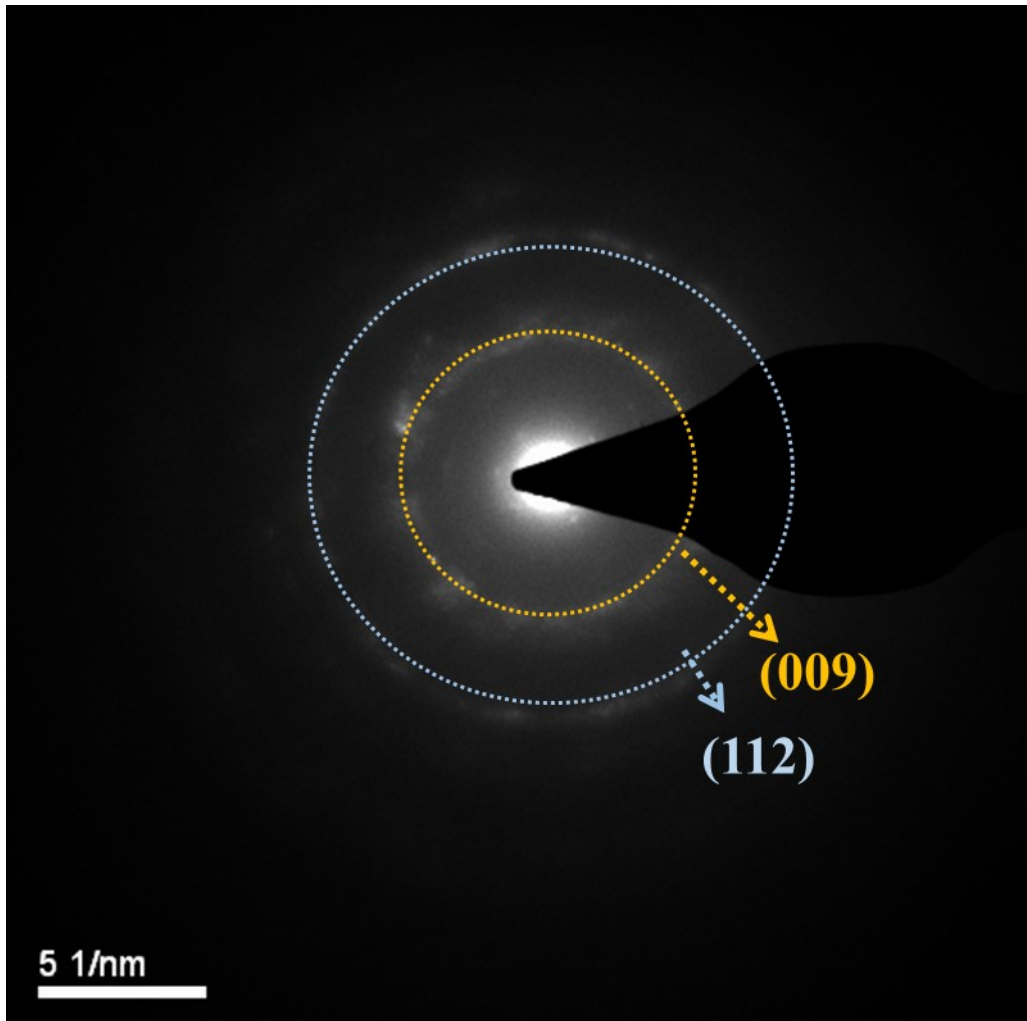


Figure S4. SAED image of $\text{Co}_{0.1}\text{Ce}_{0.01}\text{-LDH-TiO}_2\text{@C}$.

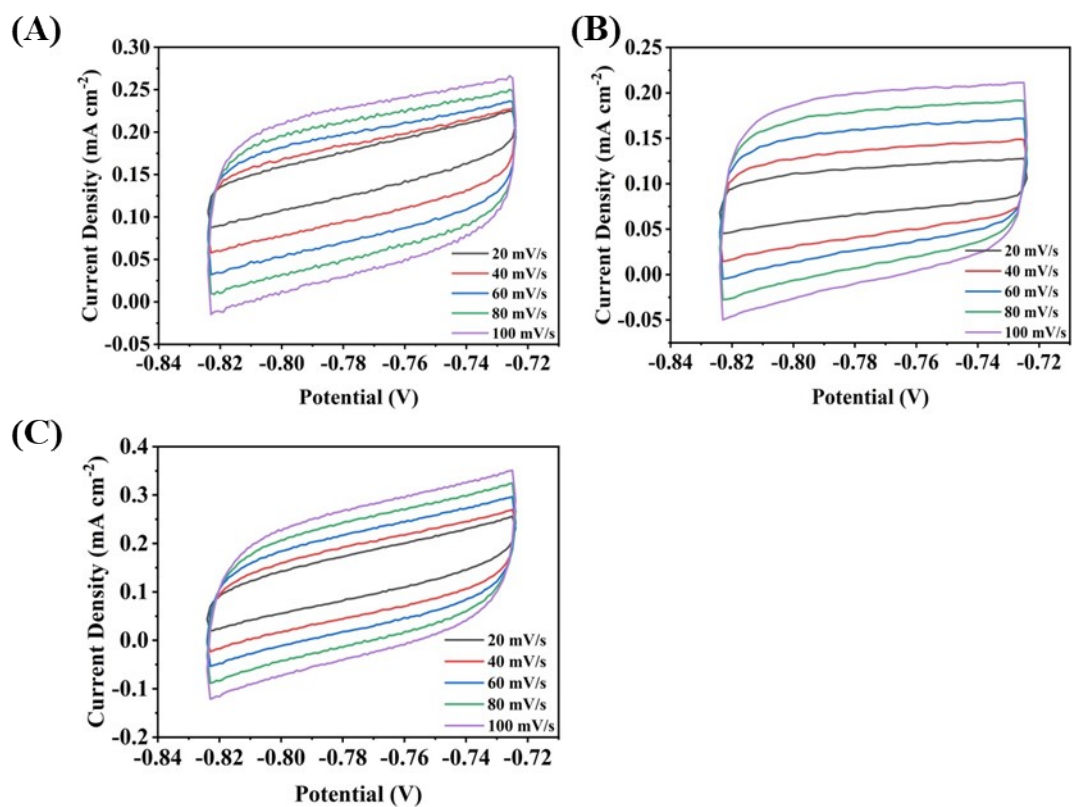


Figure S5. CV of (A) $\text{TiO}_2@\text{C}$, (B) CoCe-LDH and (C) $\text{Co}_{0.1}\text{Ce}_{0.01}\text{-LDH-TiO}_2@\text{C}$ at various scan rates for HER.

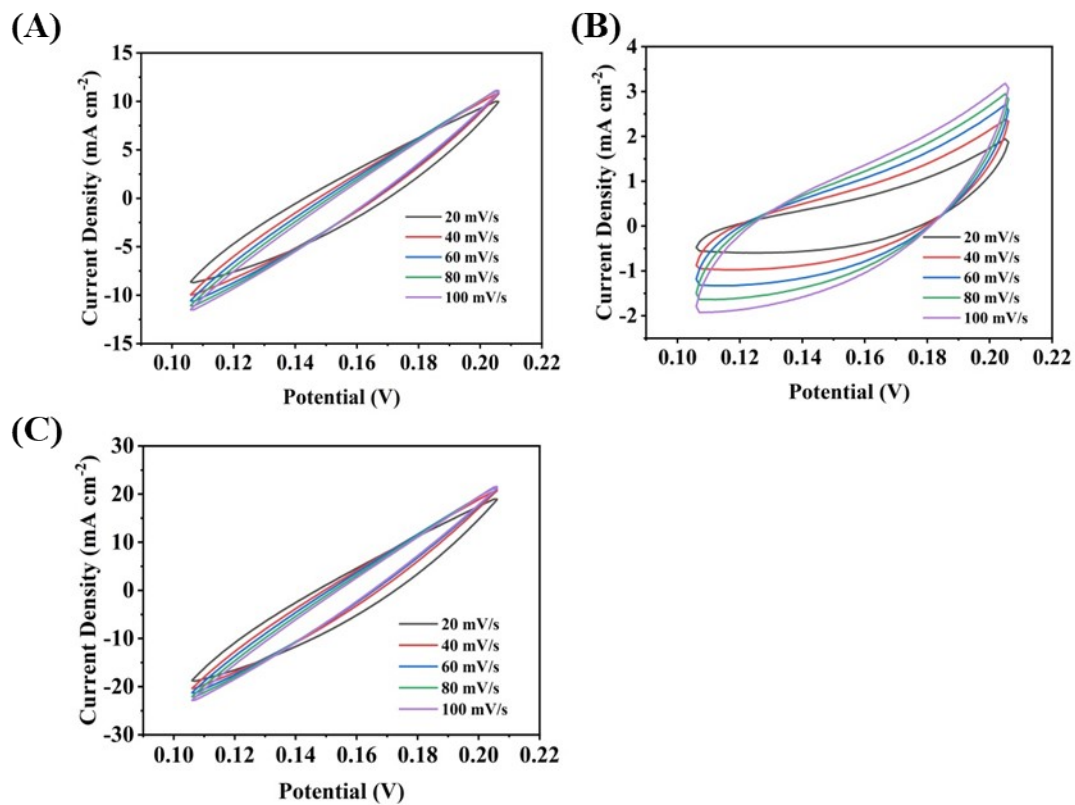


Figure S6. CV of (A) TiO₂@C, (B) CoCe-LDH and (C) Co_{0.1}Ce_{0.01}-LDH-TiO₂@C at various scan rates for OER.

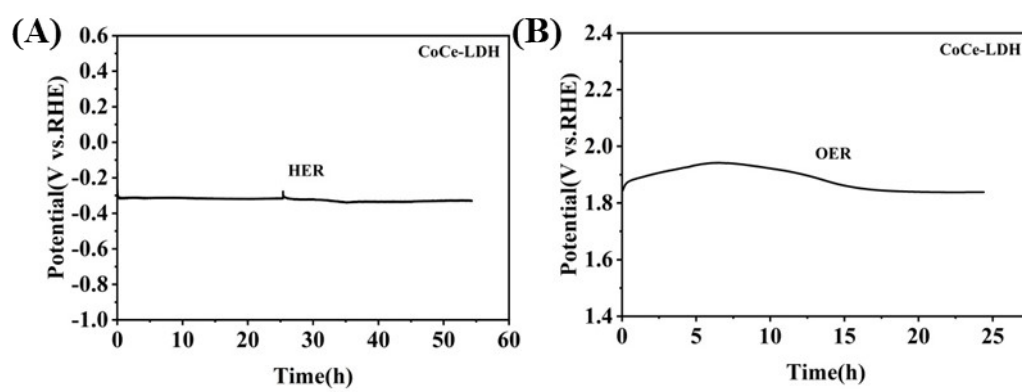


Figure S7. Chronopotentiometry measurement of CoCe-LDH of (A) HER and (B) OER performance.

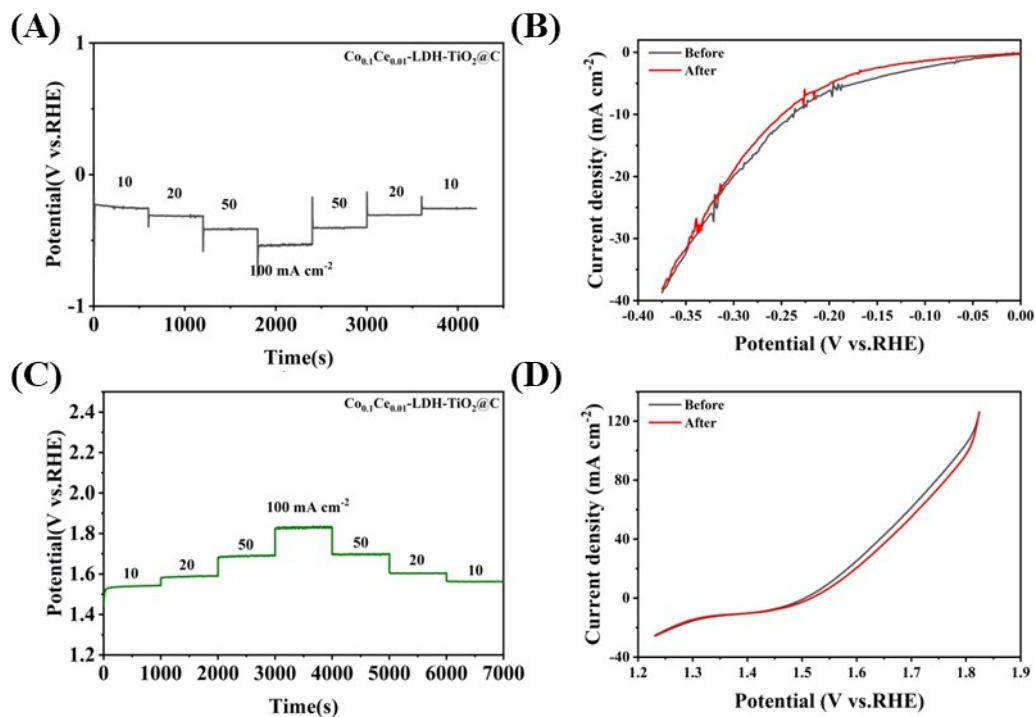


Figure S8. Stepped current stability test of $\text{Co}_{0.1}\text{Ce}_{0.01}\text{-LDH-TiO}_2\text{@C}$ for (A) HER and (C) OER, LSV curve comparison experiment before and after CV cycling of $\text{Co}_{0.1}\text{Ce}_{0.01}\text{-LDH-TiO}_2\text{@C}$ for (B) HER and (D) OER.

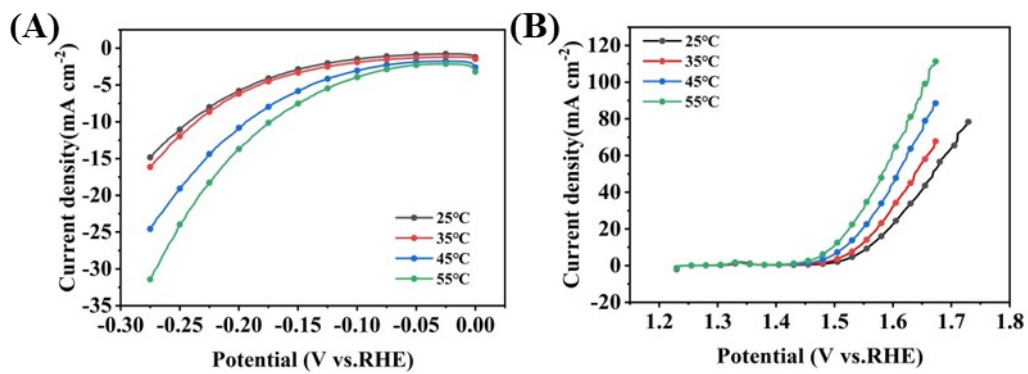


Figure S9. LSV polarization curves under different electrolyte temperatures of (A-B) CoCe-LDH.

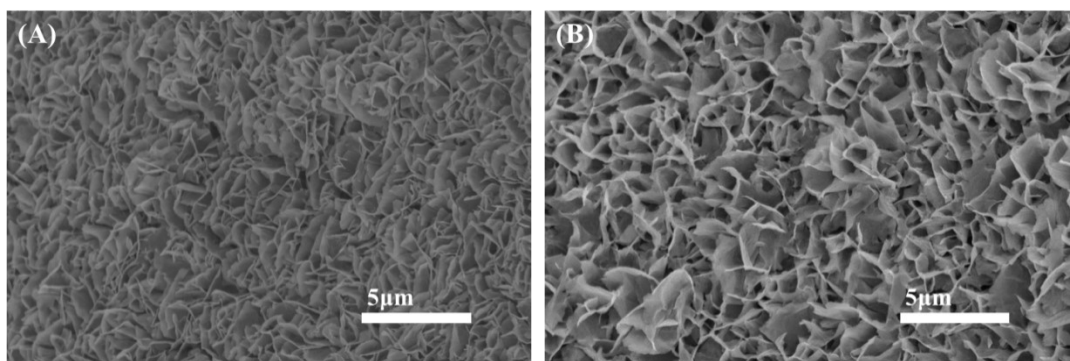


Figure S10. The SEM images of $\text{Co}_{0.1}\text{Ce}_{0.01}\text{-LDH-TiO}_2\text{@C}$ after (A) HER and (B) OER.

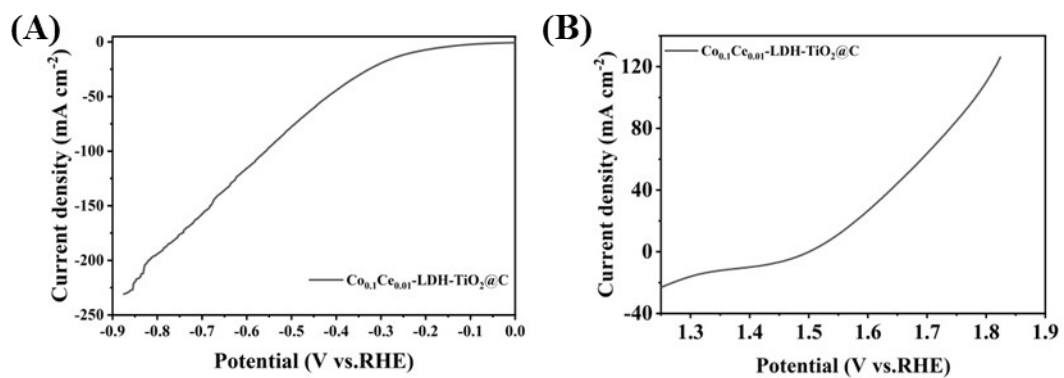


Figure S11. LSV polarization curves at high current density of $\text{Co}_{0.1}\text{Ce}_{0.01}\text{-LDH-TiO}_2\text{@C}$ for (A) HER and (B) OER.

Table S1. EIS parameters of TiO₂@C, CoCe-LDH and Co_{0.1}Ce_{0.01}-LDH-TiO₂@C at different potentials for HER.

Samples	Potential (V vs. RHE)	R_{ct} (Ω)	R_s (Ω)	CPE (mF)
TiO₂@C	-0.176 V	17.178	1.4995	0.85619
	-0.191 V	12.751	1.5959	0.87303
	-0.206 V	10.001	1.3743	0.82405
	-0.221 V	7.8108	1.1776	0.78498
	-0.236 V	6.7571	1.1382	0.75446
CoCe-LDH	-0.176 V	14.304	1.758	0.85989
	-0.191 V	10.968	1.8533	0.9105
	-0.206 V	9.0989	1.8542	0.92986
	-0.221 V	7.6343	1.8459	0.94465
	-0.236 V	6.4156	1.8839	0.94813
Co_{0.1}Ce_{0.01}-LDH-TiO₂@C	-0.176 V	6.6029	1.4359	0.6716
	-0.191 V	6.1093	1.6649	0.74449
	-0.206 V	5.6102	1.4617	0.71749
	-0.221 V	4.494	1.4968	0.74299
	-0.236 V	3.5875	1.5288	0.7842

Table S2. EIS parameters of TiO₂@C, CoCe-LDH and Co_{0.1}Ce_{0.01}-LDH-TiO₂@C at different potentials for OER.

Samples	Potential (V vs. RHE)	Rct (Ω)	Rs (Ω)	CPE (mF)
TiO₂@C	1.538 V	3.7844	1.0205	0.65756
	1.553 V	2.8462	1.0287	0.67259
	1.568 V	2.077	1.0125	0.75114
	1.583 V	1.4984	0.92555	0.7799
	1.598 V	1.3782	0.94059	0.81062
CoCe-LDH	1.538 V	3.3702	1.8442	0.82349
	1.553 V	2.4545	1.7925	0.82286
	1.568 V	1.7764	1.7896	0.83172
	1.583 V	1.3837	1.7826	0.83567
	1.598 V	1.1192	1.8153	0.84869
Co_{0.1}Ce_{0.01}-LDH-TiO₂@C	1.538 V	2.1355	1.564	0.87563
	1.553 V	1.6479	1.5679	0.86365
	1.568 V	1.2684	1.5731	0.86883
	1.583 V	0.98091	1.5844	0.88856
	1.598 V	0.84179	1.569	0.8629

Table S3. Comparison of HER and OER performance for Co_{0.1}Ce_{0.01}-LDH-TiO₂@C with other similar catalysts

Samples	η_{HER}	η_{OER}	C.D.	Ref.
Co_{0.1}Ce_{0.01}-LDH-TiO₂@C	202 mV	268 mV	10 mA cm ⁻²	This work
Co-NiFe LDH		278 mV	10 mA cm ⁻²	[1]
FeOOH(Se)/IF		287 mV	10 mA cm ⁻²	[2]
Ni/Ni(OH)₂		270 mV	10 mA cm ⁻²	[3]
Fe-CoOOH/G		330 mV	10 mA cm ⁻²	[4]
ZnCo-C/CA-PANI@NF		338 mV	10 mA cm ⁻²	[5]
NiFe-LDH(POM)		287 mV	10 mA cm ⁻²	[6].
Ir-Co₃O₄		622 mV	10 mA cm ⁻²	[18]
Co_{0.85}Se/Co₉Se₈		330 mV	10 mA cm ⁻²	[19]
NiFe-LDH/NF	210 mV		10 mA cm ⁻²	[7]
CoS/rGO	371 mV		10 mA cm ⁻²	[8].
NiCo₂S₄/NF	210 mV		10 mA cm ⁻²	[9]
Co-BDC/MoS₂	248 mV		10 mA cm ⁻²	[10]
Ni(OH)₂/MoS₂	227 mV		10 mA cm ⁻²	[11]
Dy-CuO	220 mV		10 mA cm ⁻²	[20]
CuO	243 mV		10 mA cm ⁻²	[20]
Co₃₅Cr₅Fe₁₀Ni₃₀Ti₂₀	217 mV		10 mA cm ⁻²	[21]

η_{HER} is the overpotential of HER, η_{OER} is the overpotential of OER, C.D. is current density

Table S4. Comparison of the stability performance of $\text{Co}_{0.1}\text{Ce}_{0.01}\text{-LDH-TiO}_2\text{@C}$ with other catalysts for OER.

Samples	stability performance	Ref.
$\text{Co}_{0.1}\text{Ce}_{0.01}\text{-LDH-TiO}_2\text{@C}$	100 h	This work
1T-Mn_{0.8}Ir_{0.2}O₂	75 h	[12]
NiFeMn-OOH/NF	90 h	[13]
CoP-Ni₂P@U-NCNTs/NF	48 h	[14]
Ni₂P@C	50 h	[15]
NiCoFeMoZn	50 h	[16]
PMOF-NiOOH-Ru₂₀/NF-A	50 h	[17]

Table S5. Comparison of the stability performance of $\text{Co}_{0.1}\text{Ce}_{0.01}\text{-LDH-TiO}_2\text{@C}$ with other catalysts for overall water splitting.

Samples	stability performance	Ref.
$\text{Co}_{0.1}\text{Ce}_{0.01}\text{-LDH-TiO}_2\text{@C}$	100 h	This work
$\text{IrO}_2/\text{MoS}_2$	70 h	[22]
NF-C/CoS/NiOOH	13.8 h	[23]
4N6Co-MoS₂	50 h	[24]
$\text{MS}_2/\text{RuS}_2\text{@G}$ (M=Fe,Co,Ni)	20 h	[25]
$\text{Ni}_3\text{Sb/FeSb}_2$	50 h	[26]

References

- 1 S. Si, H.-S. Hu, R.-J. Liu, Z.-X. Xu, C.-B. Wang and Y.-Y. Feng, *Int. J. Hydrogen Energy*, 2020, 45, 9368–9379.
- 2 S. Niu, W.-J. Jiang, Z. Wei, T. Tang, J. Ma, J.-S. Hu and L.-J. Wan, *J. Am. Chem. Soc.*, 2019, 141, 7005–7013.
- 3 L. Dai, Z.-N. Chen, L. Li, P. Yin, Z. Liu and H. Zhang, *Adv. Mater.*, 2020, 32, e1906915.
- 4 X. Han, C. Yu, S. Zhou, C. Zhao, H. Huang, J. Yang, Z. Liu, J. Zhao and J. Qiu, *Adv. Energy Mater.*, 2017, 7, 1602148.
- 5 M. W. Fazal, F. Zafar, M. Asad, F. Mohammad H. Al Sulami, H. Khalid, A. A. Abdelwahab, M. U. Ur Rehman, N. Akhtar, W. A. El-Said, S. Hussain and M. A. Shenashen, *ACS Appl. Energy Mater.*, 2023, 6, 2739–2746.
- 6 X. Xue, F. Yu, J.-G. Li, G. Bai, H. Yuan, J. Hou, B. Peng, L. Chen, M.-F. Yuen, G. Wang, F. Wang and C. Wang, *Int. J. Hydrogen Energy*, 2020, 45, 1802–1809.
- 7 J. Luo, J.-H. Im, M. T. Mayer, M. Schreier, M. K. Nazeeruddin, N.-G. Park, S. D. Tilley, H. J. Fan and M. Grätzel, *Science*, 2014, 345, 1593–1596.
- 8 S. Muthu, M. B. Gandhi, S. Saravanan, S. Sekar, S. Arun Kumar, P. Ilanchezhian, S. Lee and M. B. Sridharan, *Int. J. Hydrogen Energy*, 2024, 52, 1405–1414.
- 9 A. Sivanantham, P. Ganesan and S. Shanmugam, *Adv. Funct. Mater.*, 2016, 26, 4661–4672.
- 10 D. Zhu, J. Liu, Y. Zhao, Y. Zheng and S.-Z. Qiao, *Small*, 2019, 15, e1805511.
- 11 G. Zhao, Y. Lin, K. Rui, Q. Zhou, Y. Chen, S. X. Dou and W. Sun, *Nanoscale*, 2018, 10, 19074–19081.
- 12 J. Miao, H. Yu, D. Zhou, S. Li, C. Zhao, Y. Ji and Q. Shao, *Nanoscale*, 2025, 17, 21766–21775.
- 13 L. Xiao, X. Bai, J. Han, Z. Wang and J. Guan, *Cuihua Xuebao/Chin. J. Catalysis*, 2025, 71, 340–352.
- 14 N. Chen, S. Che, Y.-H. Zhang, H.-Q. Li, Y.-F. Li and X.-J. He, *Rare Metals*, 2025, 44, 4740–4755.
- 15 K. Yang, X. Liu, J. Xu, Y. Gong, S. Shen, J. Fan, X. Zhang and Y. Xue, *Prog. Nat. Sci.*, 2024, 34, 102–107.
- 16 X.-Z. Song, D.-K. Liu, X.-B. Wang, Y.-L. Meng, M.-Y. Huang, R.-C. Zhou, W.-T. Zhang, X.-F. Wang, L.-Z. Liu, J. Liang, Z. Tan and J. Liu, *J. Phys. Chem. Lett.*, 2025, 16, 9097–9106.
- 17 T. Liu, X. Yu, Y. Wu, X. Chu, W. Jiang, B. Liu, C. Liu and G. Che, *Small Methods*, 2025, 9, e2401082.
- 18 E. Easa and R. Blonder, *Chem. Educ. Res. Pract.*, 2024, 25, 1175–1196.
- 19 S. Ghosh, G. Tudu, A. Mondal, S. Ganguli, H. R. Inta and V. Mahalingam, *Inorg. Chem.*, 2020, 59, 17326–17339.
- 20 H. Wang, W. Cao, H. Sun, X. Du, Y. Wang, J. Li, L. Wu, G. Liu and S. Song, *Angew. Chem. Int. Ed Engl.*, 2026, e19688.
- 21 P. Kumari, N. Kumari, A. Priya, A. Singh, S. K. Mohapatra and R. R. Shahi, *Int. J. Hydrogen Energy*, 2025, 176, 151540.
- 22 S. Sun, Z. Wan, Y. Xu, X. Zhou, W. Gao, J. Qian, J. Gao, D. Cai, Y. Ge, H. Nie and Z. Yang, *ACS Nano*, 2025, 19, 12090–12101.
- 23 H. Wu, Q. Lu, J. Zhang, J. Wang, X. Han, N. Zhao, W. Hu, J. Li, Y. Chen and Y. Deng,

Nanomicro Lett., 2020, 12, 162.

24 Y.-Z. Lu, S.-Z. Wei, S.-S. Yang, L.-P. Fu, J.-Q. Tang, Y. Liu and W. Liu, *Tungsten*, 2025, 7, 511–524.

25 X. Zhu, M. Fang, B. Yang, S. Ke, M. Zhan, Y. Wang, S. Yang, X. Li, Y. Li and X. Min, *Small*, 2025, 21, e2412473.

26 Y. Zhang, J. Si, Z. Chen, L. Zhao, F. Qiu, W. Li, W. Zhang and S. Miao, *Adv. Energy Mater.*, 2025, 15, 2405275.